Integrating Monostatic Sensing with Communication for IoT

Zhe Chen[1], Tianyue Zheng[2], Chao Hu[3], Hangcheng Cao[4], Yanbing Yang[3], Hongbo Jiang[4], Jun Luo[2]
[1]AIWiSe, China-Singapore International Joint Research Institute, China
[2]School of Computer Science and Engineering, Nanyang Technological University, Singapore
[3]College of Computer Science, Sichuan University, China
[4]College of Computer Science and Electronics Engineering, Hunan University, China
Email: chenz@ssijri.com, {tianyue002, junluo}@ntu.edu.sg, yangyanbing@scu.edu.cn

ABSTRACT

The intention of leveraging Radio-Frequency (RF) resources for diverse sensing purposes has grown increasingly keen, thanks to the ever-expanding deployment of IoT devices using RF communications to maintain connectivity. To this end, we propose ISACoT as the framework for enabling *Integrated Sensing and Communication* (ISAC) over IoT devices. ISACoT extends over existing devices via four aspects, namely *time*, *frequency*, *space*, and *protocol*. We argue that, as the *multistatic* communication infrastructure of IoT is adverse to *device-free* sensing (e.g., lack of precise time synchronization), the keystone of ISACoT should be to operate sensing in a *monostatic* mode (like radar). We tackle the fundamental time aspect based on Wi-Fi first, then explore the other three aspects with both preliminary proposals made and potential challenges raised for future extensions.

CCS CONCEPTS

• **Hardware → Signal processing systems**; • **Human-centered computing → Ubiquitous and mobile computing systems and tools**; • **Networks** → *Wireless access networks.*

KEYWORDS

ISAC, IoT, RF sensing, monostatic sensing, Wi-Fi sensing.

ACM Reference Format:
Z. Chen, T. Zheng, C. Hu, H. Cao, Y. Yang, H. Jiang, and J. Luo. 2022. Integrating Monostatic Sensing with Communication for IoT. In *1st ACM MobiCom Workshop on Integrated Sensing and Communications Systems (ISACom '22), October 21, 2022, Sydney, NSW, Australia.* ACM, New York, NY, USA, 6 pages. https://doi.org/10.1145/3556562.3558571

1 INTRODUCTION

Internet of Things (IoT) enables a variety of "things" pervasively present around us to interact with each other [1]. Unlike the Internet, IoT is not only a data-exchanging network, but also in charge of capturing information by sensing the physical world [1]. Existing IoT often implements the two fundamental functionalities (i.e., sensing and communication) independently: sensors collect data and networks route data [19, 25]. However, the concept of IoT should not be hardened to only "networked sensors", as the *radio-frequency* (RF) communication may embrace *Integrated Sensing and Communication* (ISAC) [7] to serve sensing purposes too.

While involving specialized sensors as the front-end of IoT might be inevitable, the RF resources substantially leveraged for the (wireless) connectivity in IoT should not be neglected. In fact, *device-free sensing* exploiting a variety of RF communication devices has been heavily studied in the past [13, 14, 23], but they mostly attempt to use RF signals directly for sensing purposes without attending to the mutual interactions between sensing and communication (thus their integration). Meanwhile, many emerging IoT services call for new sensing modalities, and ISAC can cater to such needs without adding extra cost to system construction. To enable ISAC, we have to tap into the RF connectivity of spatially separated IoT nodes, which is *multistatic* in nature. However, this multistatic setting is adverse to device-free sensing for three major reasons:

Inaccurate Ranging due to Asynchrony. The synchronization protocols used by IoT often fail to correct nanosecond offsets inherent to different devices not sharing the same clocks and other processing units [15]. For example, a local oscillator not synchronized with a received carrier causes carrier frequency offset. Since 10 ns implies roughly a 3 m ranging error, the asynchrony of several nanoseconds is intolerable to sensing. This has forced existing proposals (e.g., [6, 22]) to only measure variations along or between the *line-of-sight* (LoS) and *non-line-of-sight* (NLoS) paths.

Dominating Interference from LoS Path. In a multistatic IoT network, wireless signals travel from a transmitter to a receiver via both LoS and multiple NLoS paths. Whereas the LoS path mostly carries communication data, NLoS paths are where sensing often happens. However, the LoS signal strength is much stronger and tends to overwhelm those of NLoS paths. The dominating LoS interference leads to a high quantization noise in NLoS signals [12], rendering the IoT RF signals less useful for sensing purposes.

Ambiguity in Motion Sensing. Motion sensing is another crucial capability of RF signal, as it captures the distance variation of a reflector. Due to the multistatic nature of IoT, distance variations take place along the gradient direction of the Fresnel field [26] whose contours are ellipsoids. However, since the direction of a gradient (tangent to a hyperbola) cannot be determined without knowing the reflector's range, the sensed variation magnitude can be meaningless as severe ambiguity exists in interpreting motion sensing results.

Aiming to combat the adverse effects of multistatic IoT, we propose to fundamentally overhaul IoT architecture so that sensing is conducted in *monostatic* mode: the antenna(s) of each IoT node,

ISACom '22, October 21, 2022, Sydney, NSW, Australia

ACM ISBN 978-1-4503-9525-0/22/10…$15.00
https://doi.org/10.1145/3556562.3558571

while transmitting data packets, simultaneously capture the reflected signals induced by these transmissions. Apparently, this overhaul may largely eliminate the adverse effects because i) the transmitter (Tx) and receiver (Rx) are co-located and share the same clock and processing units, ii) LoS interference disappears, and iii) sensed motion direction is well determined by the Tx and reflector regardless of the range. To fulfill these promises, ISACoT is developed to contain a novel RF front-end capable of effectively separating concurrent Tx and Rx signals. While this basic prototype enables a single IoT device to operate in an ISAC manner, several challenges remain towards a full-fledged ISACoT for all kinds of IoT devices. Therefore, we expand the exploration on ISACoT along the perspectives of *frequency*, *space*, and *protocol*, by stating the challenges and putting forward tentative solutions.

- **Bandwidth Expansion**: Modern IoT may span across multiple frequency bands, which should be better exploited to increase sensing resolution and combat interference.
- **MIMO for ISAC**: The spatial diversity introduced by the MIMO (multiple-input and multiple-output) technology is often utilized by IoT to enhance communication performance, so ISACoT needs to leverage MIMO for sensing.
- **Protocol Compatibility**: IoT encompasses a variety of wireless communication protocols, with which ISACoT needs to be integrated, better via a one-size-fits-all design.

The rest of the paper is organized as follows. We present a time-domain design of ISACoT based on Wi-Fi in Section 2. In Sections 3, 4, and 5, we respectively discuss how to expand the capabilities of ISACoT with respect to frequency, space, and protocol, accompanied by brief experiment evaluations. We finally conclude the paper in Section 6.

2 ISACoT FOR Wi-Fi: A BASIC DESIGN

We adopt Wi-Fi to implement our basic ISACoT prototype due to its wide adoption and bountiful development support.

2.1 Background on Wi-Fi Sensing

Modern Wi-Fi sensing proposals rely on CSI (channel state information) to capture signals propagation from Tx to Rx via distinct carrier frequencies and along multiple paths. Mathematically, CSI of the k-th subcarrier ($k = 0, \pm1, \pm2, \cdots$) and ℓ-th data packet can be expressed as:

$$H_\ell(k,\tau) = \sum_{p=0}^{M} \alpha_{p,\ell} e^{-j2\pi(f_c + k\Delta f)\tau_{p,\ell}}, \quad (1)$$

where M is the path cardinality, $\alpha_{p,\ell}$ and $\tau_{p,\ell}$ denote the amplitude and propagation delay along the p-th path, f_c and Δf represent the centre frequency and subcarrier spacing, respectively. In reality (see Section 1), the asynchrony between bistatic Tx and Rx results in temporal uncertainties, leading to a CSI measurement $H'_\ell(k)$ with contaminated phases:

$$H'_\ell(k,\tau) = H_\ell(k,\tau) e^{-j2\pi(\ell\gamma_c + \phi_c)} e^{-j2\pi k\beta} e^{-j2\pi k\epsilon}, \quad (2)$$

where γ_c, ϕ_c, β, ϵ denote the CFO (carrier frequency offset), CPO (carrier phase offset), SFO (sampling frequency offset), and PDD (packet detection delay), respectively. Though derived for Wi-Fi, these phase offsets apply to most IoT devices given the generic design in RF front-end. In fact, switching to the monostatic design that co-locates the Tx and Rx for sensing would naturally solve the synchronization issue, thus substantially reducing all the phase offsets. It is worth noting that, as CPO is caused by the random initialization phase, it can be changed by resetting a device and hence requires a specific calibration; we shall revisit CPO in Section 3.

2.2 Challenges to Monostatic Wi-Fi Sensing

Though adopting monostatic sensing addresses all major problems caused by the multistatic setting of Wi-Fi, the cost of removing the LoS-interference indicated by $p = 1$ in Eqn. (1) is the newly appeared Tx-interference represented by $p = 0$ in Eqn. (1); it was avoided in multistatic Wi-Fi communications by the temporal separation imposed by a MAC protocol. A naive solution to this problem is reusing the idea of *full duplex radios* (FDR) [2]. Essentially, FDR is trained under a "quiet" situation (no incoming transmissions) so that the Rx signal $R(k,\tau) = H(k,\tau)S(k)$ is purely induced by the Tx signal $S(k)$; it aims to generate a cancelling CSI H_C (both analog and digital) so as to eliminate $R(k,\tau)$, by minimizing:

$$Z(k,\tau) = H_C(k,\tau) \cdot S(k) + R(k,\tau). \quad (3)$$

Unfortunately, this FDR design does not work for ISACoT, because it removes the multipath components ($p > 1$ contained in $R(k,\tau)$) crucial to monostatic sensing.

2.3 Tx-Interference Removal for ISACoT

Our key design for ISACoT is a *Tx-Rx separator* shown in Figure 1a. This separator contains both *analog* and *digital cancellator*s. We first introduce the basic principle behind these cancellators, then we discuss their detailed constructions. Different from FDR, our separators aim to minimize only the 1st term in $Z(k,\tau)$:

$$Z(k,\tau) = \left[H_C(k,\tau)S(k) + H(k,\tau)_{p=0}S(k)\right] + H(k,\tau)_{p>1}S(k), \quad (4)$$

achieved by adding a switch to toggle between an antenna and a dummy load (shown in Figure 1b), so as to train the separator

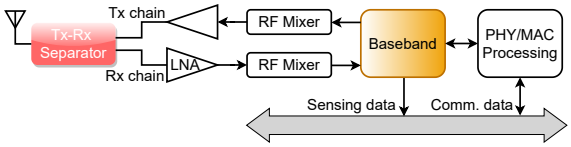

(a) ISACoT architecture: from normal switching to *separating*.

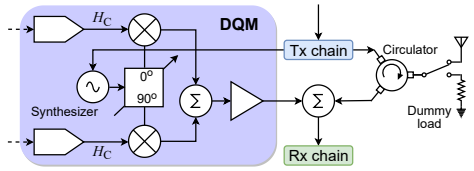

(b) Analog cancellator: an in-depth view.

Figure 1: ISACoT replaces switch with *separator* to enable concurrent Tx and Rx access (a). The key component of the separator is the *analog cancellator* (b) that mitigates Tx-interference to the Rx chain.

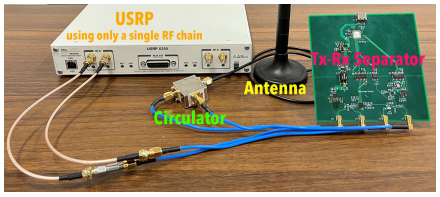

Figure 2: The USRP-based prototype of ISACoT.

under an even "quieter" situation free of the 2nd term in $Z(k,\tau)$ by switching to the dummy load.

As illustrated in Figure 1b, we adopt a direct quadrature modulator (DQM) to realize the *analog cancellator*; it is trained to approximate the inverse of $H(k,\tau)_{p=0}$ (comprised of the internal propagation path within the RF front-end) given the dummy load and thus to mitigate the 1st term in $Z(k,\tau)$. Built over USRP X310 [9] shown in Figure 2, ISACoT further contains a general purpose I/O controller to toggle an RF switch between the antenna and dummy load. Signals from antennas are first fed to a circulator to roughly split Tx and Rx, then the outcome is taken by the analog cancellator to filter the Tx-interference. The output may still have residue Tx-interference, but the dynamic range has been significantly reduced to the level that sampling it with the ADC of the USRP results in neither saturation nor large quantization errors. Consequently, the samples are taken by a digital cancellator (a programm) to further cleanse the Tx-interference. Though sharing the same principle as Eqn. (4), the *digital cancellator* differs from its analog counterpart in that H_C is trained as an adaptive filter whose coefficients are obtained via an LMS (least mean squares) algorithm.

2.4 Microbenchmarking on ISACoT

We first depict the performance of Tx-Rx separation with the Tx power set to 5dBm in Figure 3.[1] It can be observed that, while the circulator results in a 12dB reduction, the analog and digital cancellators further reduce the Tx-interference by 40dB and 25dB, respectively. The total cancellation brings the residue Tx-interference very close to the noise floor. To demonstrate the ranging and motion

[1]This choice of Tx power is rather arbitrary, as what really matters here is how much reduction can be brought by Tx-Rx separation, which is largely independent of the absolute Tx power. Moreover, this relative reduction is conditioned on the noise floor that differs from device to device; in other words, any claim on reduction below the noise floor is meaningless.

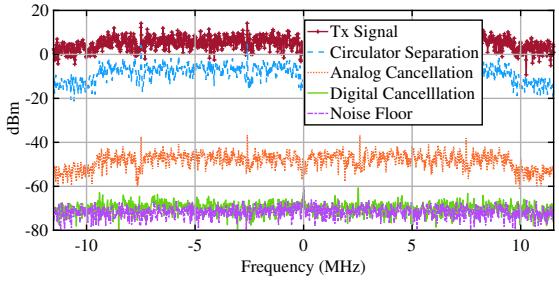

Figure 3: Power spectrum of the received baseband signal after various components of Tx-Rx separators.

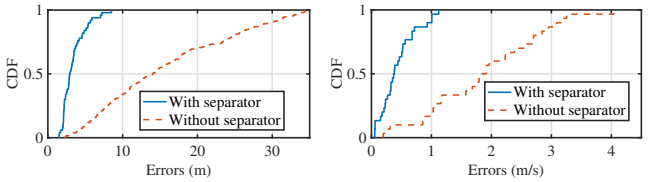

(a) Ranging errors. **(b) Speed errors.**

Figure 4: Ranging (a) and motion sensing (b) error comparisons between ISACoT and a baseline.

sensing performance of ISACoT, we take USRP without our Tx-Rx separator as the baseline, and we adopt the MUSIC algorithm [18] for parameter estimations. We fix a metal cylinder (radius 0.1 m and height 1.2 m) on a robot car and control the car remotely to move from 1 m to 15 m, with a 1 m step size in a corridor and a speed ranging from 0.6 m/s to 3.5 m/s. We obtain the ranging and speed errors shown in Figure 4a and 4b: the median ranging errors are 2.84 m and 14.14 m for ISACoT and the baseline, while median speed errors are 0.37 m/s and 1.92 m/s. Whereas the advantage of our separator is evident, the MUSIC algorithm cannot make the best out of our design, for the reason to be elaborated in Section 5.1.

3 FREQUENCY: ULTRA-WIDEBAND

Existing radar-based sensing platform leverages an ultra-wide bandwidth to achieve centimeter-level range resolution [5] (hence excellent accuracy in conducting human activity recognition [3, 8] and vital signs monitoring [4, 28]), but IoT devices do not enjoy such a luxury. Theoretically, two solutions may potentially extend ISACoT towards ultra-wideband: i) wideband Tx-interference removal and ii) channel hopping with narrowband removal for individual subbands. Whereas the former solution suffers an increasingly unstable frequency response given a growing bandwidth, the latter faces the interference from random CPOs, ϕ_c in Eqn. (2), after each hopping. In practice, relying on wideband IoT is nearly impossible because certain channels may not be available when in need. Therefore, we decide to leverage channel hopping to utilize discontinuous but idle channels, by rising to the challenge of calibrating CPOs.

Channel Hopping Calibration. To calibrate the CPOs caused by channel hopping, we rewrite the Rx phase of the k-th subcarrier (within the i-th channel with centre frequency f_c^i) and ℓ-th packet in Eqn. (2) as $\psi_{i,k,\ell} = \delta_{i,k,\ell} + \phi_c^i$, where $\delta_{i,k,\ell} = 2\pi(f_c^i + k\Delta f)\tau_{p,\ell}$ denotes the phase caused by a physical channel. We propose to leverage a *two-way* transmission along the circuit to cancel $\delta_{i,k,\ell}$. Basically, after each channel hopping, both Tx and Rx chains are toggled to a short circuit and then transmit to each other. We have $\psi^{\text{Tx}}_{i,k,\ell} = \delta_{i,k,\ell} + \phi_c^i$ when the Tx chain transmits and $\psi^{\text{Rx}}_{i,k,\ell} = \delta_{i,k,\ell} - \phi_c^i$ otherwise. This allows the CPO to be calibrated as $\phi_c^i = \left(\psi^{\text{Tx}}_{i,k,\ell} - \psi^{\text{Rx}}_{i,k,\ell}\right) \Big/ 2$.

Sparse Recovery for Non-Continuous Channels. After the CPO calibration, we obtain a *CSI tensor* $H_\ell(i,k,\tau)$ whose individual components $H_\ell(k,\tau)$ are CSI matrices for respective channels. To estimate the delay $\tau_{p,\ell}$ under discontinuous channels, we formulate

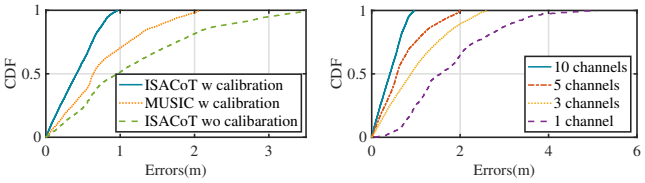

(a) CPO calibration. (b) Number of channels.

Figure 5: Ranging performance of wideband sensing.

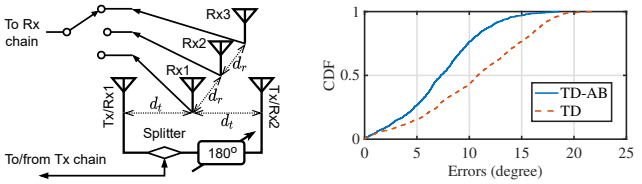

(a) Antenna architecture. (b) CDF of AoA errors.

Figure 6: A hybrid TD-AB ISAC-MIMO for ISACoT.

the problem as a sparse optimization:

$$\min \|\mathbf{q}\|_1 \tag{5}$$

$$\text{s.t.} \quad \left\| \Sigma_{i=1}^{I} \Sigma_{k=1}^{K} H_\ell(k,\tau) - z(\hat{\alpha},\hat{\tau}) \right\|_2 = 0, \tag{6}$$

$$z(\hat{\alpha},\hat{\tau}) = \Sigma_{i=1}^{I} \Sigma_{k=1}^{K} \Sigma_{p=1}^{M} \hat{\alpha}_{p,\ell} e^{-j2\pi(f_c^i + k\Delta f)\hat{\tau}_{p,\ell}},$$

where $\mathbf{q} = [\hat{\alpha}_{1,\ell}, \hat{\alpha}_{2,\ell}, \cdots, \hat{\alpha}_{M,\ell}, \hat{\tau}_{1,\ell}, \hat{\tau}_{2,\ell}, \cdots, \hat{\tau}_{M,\ell}]^T$, $\|\cdot\|_1$ and $\|\cdot\|_2$ refer to L^1 and L^2 norms, respectively. We conduct experiments to validate these solutions using the setting in Section 2.4, with 10 arbitrary 20Mhz channels in the range from 5.160GHz to 5.885GHz for ISACoT and MUSIC [18] as the baseline. The results illustrated in Figure 5a show median errors of 0.41m and 0.95m respectively for ISACoT with and without calibration (resp. wc and woc), while that of the baseline (0.65m) is worse than ISACoT-wc, because our algorithm refines its estimation with multiple iterations. We also show the performance improvement of ISACoT-wc while increasing channel numbers from 1 to 10 in Figure 5b.

4 SPACE: MIMO SENSING

Acquiring a finer spatial resolution demands MIMO sensing with multiple antennas, whose design entails a much higher degree of freedom, hence offering more opportunities.

4.1 Approaching ISAC-MIMO

Three major architectures exist to enable ISAC-MIMO, namely time-division, digital beamforming, and analog beamforming [5]. *Time-Division* (TD) MIMO enforces different antennas to be in Tx/Rx states at non-overlapping time slots; it is cheap and easy to implement, but it incurs non-negligible time delays. *Digital Beamforming* (DB) employs multiple RF chains each equipped with a single antenna. It transmits or receives signals simultaneously, and hence has the most flexible and fast beam steering capability. Unfortunately, large-scale DB can be too costly for IoT devices. *Analog Beamforming* (AB) consists of two RF chains (respectively for Tx and Rx similar to TD) each with multiple antennas driven by phase shifters (a.k.a. phased antenna array). It selects different beamforming patterns (via different phase shifter paths) to steer Tx and Rx towards pre-defined directions. Apparently, AB's performance and cost sit between TD and DB, and building high quality shifters can be highly nontrivial.

4.2 A Preliminary TD Implementation

We choose to realize a preliminary ISAC-MIMO implementation based on a hybrid TD-AB architecture with two RF chains: one for Tx (and concurrent Rx enabled by the Tx-Rx separator introduced in Section 2.3) while another for pure Rx. Since our separator is calibrated only for internal Tx-interference within a chain circuit, it may not properly handle the interference cancellation across different chains. Consequently, we exploit the phase cancellation idea of a simple AB architecture. As illustrated in Figure 6a, the *Tx chain* retrofits the right side of the circulator in Figure 1 to drive two symmetrically placed antennas via a (phase) splitter, and the *Rx chain* employs a switch to receive from three Rx antennas separated by half wavelength d_r. These five antennas are strategically placed so that the axis of the later three is perpendicular to that of the first two, so that the 180° phase splitter causes the Tx-interference to have a zero sum at the Rx chain. We verify the performance of this design by placing a rotary robot 1.5m from ISACoT with six different bearings: 0°, 30°, 45°, 60°, 75°, 90°. We apply MUSIC to estimate the AoA (angle of arrival) and compare the two designs with and without the phase splitter. According to Figure 6b, it is evident that the simple AB upgrade (with its phase cancellation) outperforms the one without it, since the cross-chain interference is better suppressed.

4.3 Challenges to ISAC-MIMO

Our hybrid TD-AB design is only a taste of ISAC-MIMO, so it leaves plenty of challenges for further studies.

From Hybrid to AB MIMO. Our preliminary design incurs a technical issue: a target close to the axis of the Rx antennas can barely be detected due to the mutual cancellation of the two Tx signals, and the sensing resolution can be affected by the distance between the target and the axis. While a direct solution to this issue is adopting phased antenna array for the Tx chain to avoid the "dead angle", switching to pure AB MIMO implementation may yield a much better spatial resolution leveraging the beam scanning algorithms used for mmWave sensing [11, 16, 20]. Nonetheless, how to suppress cross-chain Tx-interference via intelligent beamforming scheduling remains to be a challenge.

Aliasing Layout MIMO. Instead of the expensive phased array, specially designed TD antenna layout is much cheaper while avoiding the cross-chain interference by relying on only one RF chain. Consider the equally spaced antennas in our preliminary design, the spacing sequence of the *virtual array* becomes $[0, 2d_r, 2d_r]$ [21]. Since this layout leads to aliasing beamforming patterns preventing a target to be distinguished, we upgrade it with a special strategy where the spacing sequence of physical and virtual arrays are respectively set as $[0, d_r/2, d_r]$ and $[0, d_r, 2d_r]$. Consequently, one

anti-aliasing and two alisasing beamforming patterns are generated by three antennas pairwisely, thus a target can be detected by combining these patterns. However, this layout may not handle nearby targets with only one anti-aliasing pattern, and it can be too strict for hardware design.

Large-scale DB MIMO. If cost is not an issue, large-scale (i.e., more than 10 antennas in an array [24]) DB MIMO can be adopted to deliver high spatial resolution; it may even drop the need for the analog cancellator shown in Figure 1b, by leveraging part of its RF chains (hence antennas) to transmit phase-complementing signals and hence to null the cross-chain Tx-interference at the remaining Rx chains [10]. However, as the Tx-interference is blended with the reflected signals (similar to the FDR situation in Section 2.2), DB MIMO may face challenges in acquiring qualified monostatic sensing information. One may argue for a directional beamforming solution to avoid the cross-chain interference (as opposed to the above nulling scheme), yet this virtually degenerates DB to AB; we hence leave a new beamforming algorithm design for DB ISAC-MIMO as another challenge.

5 TOWARDS GENERALIZED ISACoT

We herein discuss two levels of protocol compatibility for ISACoT: i) between sensing and communication and ii) with other IoT protocols beyond Wi-Fi.

5.1 Communications during Sensing

Although our Tx-Rx separator allows for currently sensing and communication at hardware level, the resulting hardware operations may not be compatible with Wi-Fi at protocol level. As shown in Figure 7, applying the Tx-Rx separator during normal packet receptions significantly reduces SNR and hence throughput: because the MAC protocol prohibits Tx from transmitting, the separator is reduced to a noise-driven filter. In fact, it is a waste of computing resource to apply the Tx-Rx separator on normal Rx signals. In addition, as normal Wi-Fi traffic contains a series of irregular packets, the sequence of CSIs contained in the reflected Rx signals are also irregular. As a result, existing Wi-Fi sensing approaches that implicitly assume regular CSI receptions [17, 22] may fail to achieve an adequate performance. We conduct experiments with the rotary robots and 80 MHz bandwidth (similar settings already adopted in Section 3): under irregular CSI receptions, the FFT baseline algorithm barely delivers a reasonable resolution due to the dispersed energy, as shown in Figure 8a upper panel.

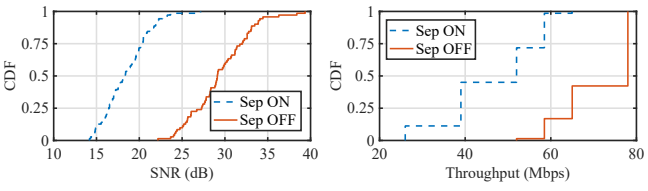

(a) SNR. (b) Throughput.

Figure 7: The Tx-Rx separator (Sep) heavily degrades normal Wi-Fi packet reception quality.

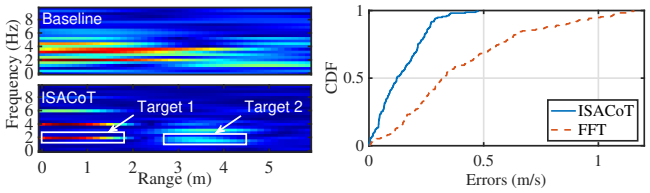

(a) Examples. (b) Speed errors.

Figure 8: Motion sensing performance comparison between ISACoT and FFT baseline under irregular CSI receptions: (a) range-frequency heatmap and (b) speed estimation error.

To avoid interfering normal receptions, we propose and implement a minor yet critical revision to the MAC protocol. In particular, ISACoT starts with a C-state (for communications), and a DATA or ACK message invokes the transition to an M-state (for monostatic sensing), which respectively activates the analog and digital cancellators by a hardware interrupt and a function call. A transition back from the M-state to the C-state is controlled by a timer fine-tunable to suit surrounding environments. As for handling the irregular CSI receptions, we leverage NFFT (non-uniform fast Fourier transform) to enhance the sparse optimization framework introduced in Section 3. As shown in Figure 7, switching off the separator before packet reception does significantly improve the performance of Wi-Fi communications. In addition, our NFFT enhanced sparse optimization enables ISACoT to achieve speed estimation accuracy far more superior to that achieved by the FFT baseline algorithm, as shown in both Figure 8a lower panel and 8b.

5.2 ISAC beyond Wi-Fi

The final target of ISACoT is aiming for a general and protocol-free ISAC architecture. Because it is a non-trivial task to tackle all kinds of IoT devices in one paper, we only lay down a few opportunities and challenges.

One-Size-Fits-All Design. Though ISACoT is currently designed only Wi-Fi, its plug-and-play and protocol-independent architecture should allow it to be smoothly migrated to other IoT protocols for two reasons. On one hand, ISACoT only utilizes CSIs for sensing while almost all IoT protocols offer such a feature in their firmware. On the other hand, the frequency range of ISACoT coincides with most IoT protocols. Interestingly, we also find that certain modulations, e.g., chirp spread spectrum adopted by LoRa, may help improving the Tx-interference suppression, since frequency modulation scheme concentrates energy into a single frequency component at any given point in time, standard low pass filter may be sufficient to handle Tx-interference.

Encompassing Other Sensing Modes. In fact, ISACoT does not have to be confined to only monostatic sensing mode; it is certainly compatible with the well-studied multistatic sensing mode [13, 14, 23]. This is because, when bypassing the Tx-interference separator under the C-state, an IoT device simply works under the normal communication mode and multistatic sensing can directly piggyback on it, while exploiting our proposals on bandwidth expansion

(Section 3) and protocol compatibility (Section 5.1) to improve sensing performance. Combining monostatic sensing with multistatic sensing should significantly expand the distributed collaborative sensing involving many IoT devices.

6 CONCLUSION

Bearing the ambition of making all IoT devices ISAC-ready, we propose ISACoT as a general framework encompassing time, frequency, space, protocol aspects of the problem. While our preliminary prototype has largely addressed the time domain aspect of ISACoT under Wi-Fi, we are still on the way to extending it towards wider bandwidth, higher spatial diversity, and broader protocol compatibility. We present our preliminary studies and implementations for each aspect, while leaving a few critical issues as challenges, expecting our research community to join forces in fully tackling them. In summary, we have raised the following challenges to ISACoT: i) distributed collaborative sensing, ii) bandwidth expansion, iii) MIMO implementation, and iv) compatible with general IoT protocols. Currently, we are working towards tackling all the challenges raised in this paper, as well as combining our ISACoT framework with the novel signal processing techniques enabled by deep learning [27] for improving the performance for both sensing and communications

REFERENCES

[1] Kevin Ashton. 2009. That 'Internet of Things' Thing. *RFID Journal* 22, 7 (2009), 97–114.

[2] Dinesh Bharadia, Emily McMilin, and Sachin Katti. 2013. Full Duplex Radios. In *Proc. of the 27th ACM SIGCOMM*. 375–386.

[3] Zhe Chen, Chao Cai, Tianyue Zheng, Jun Luo, Jie Xiong, and Xin Wang. 2021. RF-Based Human Activity Recognition Using Signal Adapted Convolutional Neural Network. *IEEE Trans. on Mobile Computing* (2021), 1–13.

[4] Zhe Chen, Tianyue Zheng, Chao Cai, and Jun Luo. 2021. MoVi-Fi: Motion-robust Vital Signs Waveform Recovery via Deep Interpreted RF Sensing. In *Proc. of the 27th ACM MobiCom*. 392–405.

[5] Zhe Chen, Tianyue Zheng, and Jun Luo. 2021. Octopus: A Practical and Versatile Wideband MIMO Sensing Platform. In *Proc. of the 27th ACM MobiCom*. 601–614.

[6] Zhe Chen, Guorong Zhu, Sulei Wang, Yuedong Xu, Jie Xiong, Jin Zhao, Jun Luo, and Xin Wang. 2021. M^3: Multipath Assisted Wi-Fi Localization with a Single Access Point. *IEEE Trans. on Mobile Computing* 20, 2 (2021), 588–602.

[7] Yuanhao Cui, Fan Liu, Xiaojun Jing, and Junsheng Mu. 2021. Integrating Sensing and Communications for Ubiquitous IoT: Applications, Trends, and Challenges. *IEEE Network* 35, 5 (2021), 158–167.

[8] Shuya Ding, Zhe Chen, Tianyue Zheng, and Jun Luo. 2020. RF-Net: A Unified Meta-Learning Framework for RF-enabled One-Shot Human Activity Recognition. In *Proc. of the 18th ACM SenSys*. 517–530.

[9] Ettus Research. 2014. USRP X310 High Performance Software Defined Radio - Ettus Research. https://www.ettus.com/all-products/x310-kit/. Online; accessed 26 February 2022.

[10] Evan Everett, Clayton Shepard, Lin Zhong, and Ashutosh Sabharwal. 2016. SoftNull: Many-Antenna Full-duplex Wireless via Digital Beamforming. *IEEE Transactions on Wireless Communications* 15, 12 (2016), 8077–8092.

[11] Yasaman Ghasempour, Muhammad K. Haider, Carlos Cordeiro, Dimitrios Koutsonikolas, and Edward Knightly. 2018. Multi-Stream Beam-Training for MmWave MIMO Networks. In *Proc. of the 24th ACM MobiCom*. 225–239.

[12] Daniel Chaim Halperin. 2013. Simplifying the Configuration of 802.11 Wireless Networks with Effective SNR. *arXiv preprint arXiv:1301.6644* (2013).

[13] Haotian Jiang, Jiacheng Zhang, Xiuzhen Guo, and Yuan He. 2021. Sense Me on the Ride: Accurate Mobile Sensing over a LoRa Backscatter Channel. In *Proc. of the 19th ACM SenSys*. 125–137.

[14] Wenjun Jiang, Chenglin Miao, Fenglong Ma, Shuochao Yao, Yaqing Wang, Ye Yuan, Hongfei Xue, Chen Song, Xin Ma, Dimitrios Koutsonikolas, Wenyao Xu, and Lu Su. 2018. Towards Environment Independent Device Free Human Activity Recognition. In *Proc. of the 24th ACM MobiCom*. 289–304.

[15] Manikanta Kotaru, Kiran Joshi, Dinesh Bharadia, and Sachin Katti. 2015. SpotFi: Decimeter Level Localization Using WiFi. In *Proc. of 29th ACM SIGCOMM*. 269–282.

[16] Joan Palacios, Daniel Steinmetzer, Adrian Loch, Matthias Hollick, and Joerg Widmer. 2018. Adaptive Codebook Optimization for Beam Training on Off-the-Shelf IEEE 802.11ad Devices. In *Proc. of the 24th ACM MobiCom*. 241–255.

[17] Kun Qian, Chenshu Wu, Yi Zhang, Guidong Zhang, Zheng Yang, and Yunhao Liu. 2018. Widar2.0: Passive Human Tracking with a Single Wi-Fi Link. In *Proc. of the 16th ACM MobiSys*. 350–361.

[18] R. Schmidt. 1986. Multiple Emitter Location and Signal Parameter Estimation. *IEEE Trans. on Antennas and Propagation* 34, 3 (1986), 276–280.

[19] Eugene Siow, Thanassis Tiropanis, and Wendy Hall. 2018. Analytics for the Internet of Things: A Survey. *ACM Computing Surveys (CSUR)* 51, 4 (2018), 1–36.

[20] Sanjib Sur, Ioannis Pefkianakis, Xinyu Zhang, and Kyu-Han Kim. 2018. Towards Scalable and Ubiquitous Millimeter-Wave Wireless Networks. In *Proc. of the 24th ACM MobiCom*. 257–271.

[21] Texas Instruments. 2018. MIMO Radar. https://www.ti.com/lit/an/swra554a/swra554a.pdf?ts=1646987111261&ref_url=https%253A%252F%252Fwww.ti.com%252Fproduct%252FAWR1843. Online; accessed 26 February 2022.

[22] Ju Wang, Hongbo Jiang, Jie Xiong, Kyle Jamieson, Xiaojiang Chen, Dingyi Fang, and Binbin Xie. 2016. LiFS: Low Human-Effort, Device-Free Localization with Fine-Grained Subcarrier Information. In *Proc. of the 22nd ACM MobiCom*. 243–256.

[23] Teng Wei, Shu Wang, Anfu Zhou, and Xinyu Zhang. 2015. Acoustic Eavesdropping through Wireless Vibrometry. In *Proc. of the 21st MobiCom*. 130–141.

[24] Qing Yang, Xiaoxiao Li, Hongyi Yao, Ji Fang, Kun Tan, Wenjun Hu, Jiansong Zhang, and Yongguang Zhang. 2013. BigStation: Enabling Scalable Real-time Signal Processingin Large MU-MIMO Systems. *ACM SIGCOMM Computer Communication Review* 43, 4 (2013), 399–410.

[25] Jennifer Yick, Biswanath Mukherjee, and Dipak Ghosal. 2008. Wireless Sensor Network Survey. *Computer Networks* 52, 12 (2008), 2292–2330.

[26] Fusang Zhang, Daqing Zhang, Jie Xiong, Hao Wang, Kai Niu, Beihong Jin, and Yuxiang Wang. 2018. From Fresnel Diffraction Model to Fine-Grained Human Respiration Sensing with Commodity Wi-Fi Devices. *Proc. ACM Interact. Mob. Wearable Ubiquitous Technol.* (2018), 53:1–23.

[27] Tianyue Zheng, Zhe Chen, Shuya Ding, and Jun Luo. 2021. Enhancing RF Sensing with Deep Learning: A Layered Approach. *IEEE Communications Magazine* 59, 2 (2021), 70–76.

[28] Tianyue Zheng, Zhe Chen, Shujie Zhang, Chao Cai, and Jun Luo. 2021. MoRe-Fi: Motion-robust and Fine-grained Respiration Monitoring via Deep-Learning UWB Radar. In *Proc. of the 19th ACM SenSys*. 111–124.